EUROPEAN UROLOGY 75 (2019) 329–340

available at www.sciencedirect.com
journal homepage: www.europeanurology.com

European Association of Urology

Sexual Medicine

Antifibrotic Synergy Between Phosphodiesterase Type 5 Inhibitors and Selective Oestrogen Receptor Modulators in Peyronie's Disease Models

Marcus M. Ilg[a], *Marta Mateus*[a], *William J. Stebbeds*[b], *Uros Milenkovic*[c], *Nim Christopher*[d], *Asif Muneer*[d,e,f], *Maarten Albersen*[c], *David J. Ralph*[d,f], *Selim Cellek*[a,*]

[a] *Anglia Ruskin University, Chelmsford, UK;* [b] *Cranfield University, UK;* [c] *KU Leuven, Leuven, Belgium;* [d] *University College London Hospital, London, UK;* [e] *NIHR Biomedical Research Centre, University College London Hospital, London, UK;* [f] *University College London, London, UK*

Article info

Article history:
Accepted October 4, 2018

Associate Editor:
Jean-Nicolas Cornu

Keywords:
Peyronie's disease
Fibroblast
Myofibroblast
Fibrosis
Fibroproliferative
Phosphodiesterase type 5 inhibitor
Oestrogen receptor modulator
Tunica albuginea
Phenotypic screening

Abstract

Background: Peyronie's disease (PD) is a fibrotic disorder of the penile tunica albuginea, characterised by the formation of a localised fibrous plaque that can lead to deformity and erectile dysfunction. Nonsurgical therapeutic options for PD are limited in efficacy and safety. Myofibroblasts are key cells in the pathogenesis of PD, and inhibition of myofibroblast transformation has been suggested as a therapeutic option.
Objective: To identify potential drugs using a novel phenotypic assay and then to test them using in vitro and in vivo models of PD.
Design, setting, and participants: We have developed and validated a phenotypic screening assay that measures myofibroblast transformation, by which we tested 21 compounds that were suggested to be efficacious in treating PD. The successful hits from this assay were further tested using in vitro and in vivo models of PD.
Results and limitations: The new assay was able to detect transforming growth factor-β1–induced myofibroblast transformation. Using this assay, phosphodiesterase type 5 inhibitors (PDE5i) and selective oestrogen receptor modulators (SERMs) were identified to significantly inhibit myofibroblast transformation. A PDE5i (vardenafil) and an SERM (tamoxifen) inhibited myofibroblast transformation, collagen gel contraction, and extracellular matrix production in a synergistic fashion. In a rat model of PD, the antifibrotic effect of the combination of vardenafil and tamoxifen was greater than that of each drug alone. This study is limited by not providing a molecular mechanism for the proposed synergy.
Conclusions: This is the first demonstration of a synergistic activity between a PDE5i and an SERM discovered through a phenotypic screening approach. Future clinical trials using a combination of these drugs should be considered during the active phase of PD, given the early evidence of benefit in both in vitro and in vivo models.
Patient summary: This report suggests that the combination of a phosphodiesterase type 5 inhibitor and a selective oestrogen receptor modulator may be efficacious in treating Peyronie's disease in its active phase.

* Corresponding author. Medical Technology Research Centre, Faculty of Health, Education, Medicine and Social Care, Anglia Ruskin University, Bishop Hall Lane, Chelmsford, Essex, CM1 1SQ, UK.
E-mail address: selim.cellek@anglia.ac.uk (S. Cellek).

https://doi.org/10.1016/j.eururo.2018.10.014

1. Introduction

Peyronie's disease (PD) is a fibrotic disorder characterised by the formation of a fibrous plaque in the connective tissue surrounding the penile erectile tissue, the tunica albuginea (TA). It is a benign condition of unknown aetiology characterised by the formation of localised fibrous plaques, resulting in a penile deformity, manifesting as a curvature, indentation, or shortening during erection. The disease has been shown to be prevalent, especially as men get older [1], and affects quality of life, principally through pain during erection, erectile dysfunction, loss of penetrative ability during intercourse, and associated psychological stress [2,3]. Despite the progress in understanding the pathophysiology of PD, there is currently a lack of efficacious medical therapies for PD, with surgery or collagenase injections [4] being the main treatment options. Although the surgical outcomes following penile straightening are well documented, surgery is invasive, costly, and frequently detrimental to penile size and erectile function [5].

Myofibroblasts have the features of both fibroblasts and smooth muscle cells, and are characterised by the presence of alpha-smooth muscle actin (α-SMA)-positive cytoplasmic fibres. These actin fibres contribute to the contractile ability of these cells [6]. Although various progenitor cells for myofibroblasts have been suggested [7], they most often differentiate from locally residing fibroblasts through normal wound healing signalling, particularly transforming growth factor-β1 (TGF-β1) [8]. Myofibroblasts have been shown to play vital and ubiquitous roles in both normal wound healing and fibrosis. Most important functions include production and remodelling of extracellular matrix (ECM) protein [6,9], and secretion of profibrotic and proinflammatory cytokines [9]. These cells have been shown to be present in liver [10], lung [11], and kidney [12] fibrosis as well as in PD plaques [13,14]. It is therefore generally agreed that myofibroblasts play a critical role in the pathophysiology of fibrosis. Since the inhibition of myofibroblast transformation has been shown to be effective in preventing fibrosis [15], we aimed to identify whether compounds that are suggested for the treatment of PD can inhibit myofibroblast formation using a phenotypic screening assay. Here, we report the development of such a phenotypic screening assay through which we identified two classes of drugs, phosphodiesterase type 5 inhibitors (PDE5i) and selective oestrogen receptor modulators (SERM), which were shown to synergise in both in vitro and in vivo studies.

We first developed a phenotypic screening assay that is capable of reproducibly measuring transformation of human primary TA-derived fibroblasts to myofibroblasts in a high-throughput format. We then tested 21 compounds/drugs that have been suggested to be efficacious in in vitro, in vivo animal, and human studies of PD. We identified two classes of drugs, PDE5i and SERMs, from that screen and further tested them alone or in combination in in vitro and in vivo models of PD.

2. Patients and methods

2.1. Acquisition of TA samples and isolation of fibroblasts

TA tissue samples were collected from patients undergoing surgery at University College London Hospital (UCLH), London, UK, for penile cancer or PD. All patients gave fully informed written consent to the study. This study was approved by independent research ethics committees (NRES Committee East of England 12/EE/0170 and NRES Committee North of Scotland 15/NS/0051). PD plaque tissue was obtained from patients with chronic PD undergoing a Lue procedure (plaque incision and grafting). Plaque tissue would have otherwise been discarded. Nonplaque TA was obtained from PD patients undergoing a Nesbit procedure whereby nonfibrotic TA tissue was excised from the opposite side of the plaque. TA tissue samples from patients with penile cancer were taken from the proximal side away from the tumour, with the tumour showing negative margins on histological examination.

Tissue samples were carefully dissected to ensure that all cavernosal tissue was removed from the TA. To establish fibroblast cultures, TA fragments were seeded in six-well tissue culture plates (Fisher Scientific, Loughborough, United Kingdom) as described previously [16]. The tissue pieces were incubated in DMEM-F12 (GIBCO, Invitrogen, Waltham, Massachusetts, United States) containing 10% FCS (Fisher Scientific) and 1% penicillin-streptomycin (GIBCO, Invitrogen) at 37 °C and 5% CO_2, for 5–7 d. Tissue fragments were carefully removed using forceps upon outgrowth of cells. Passages 2–4 were used for the rest of the experiments.

2.2. In-cell enzyme-linked immunosorbent assay

Cells were seeded onto 96-well, optical, flat-bottom, black microplates (Nunc, Fisher Scientific) at 5×10^3 cells/well. After overnight attachment, they were incubated with or without 10 ng/ml TGF-β1 for 72 h. The cells were then fixed using 4% paraformaldehyde, and blocked with 10% donkey serum and 0.1% Triton X-100 in phosphate-buffered saline (PBS). The cells were then incubated with anti–α-SMA antibody (1:3000; Sigma-Aldrich, Gillingham, United Kingdom) for 2 h. Afterwards cells were incubated with donkey antimouse secondary antibody conjugated to an infrared dye that emits at 800 nm (1:500; IRdye 800CW; Li-COR, Cambridge, United Kingdom) and a nuclear counterstain at that emits at 700 nm (1:1000; DRAQ5; Biostatus, Loughborough, United Kingdom) for 1 h. The plate was scanned using an infrared imaging system (Odyssey CLx imager; LI-COR) at both 700 and 800 nm wavelengths.

2.3. Collagen gel contraction assay

A cell contraction assay (CBA-201; Cell Biolabs Inc., San Diego, California, United States) was used according to the manufacturer's instructions. Briefly, 10 000 cells/well were mixed with collagen solution and DMEM with or without 10 ng/ml TGF-β1, and then plated onto 96-well plates. Cultures were incubated for 3 d at 37 °C, at 5% CO_2, and lattices were released from the walls of the wells using a sterile spatula or needle. Contraction of the collagen lattices was observed for 8 h and documented using a digital camera (Canon Digital IXUS 55, 5.0 mega pixels). Images were analysed using ImageJ software by measuring the surface area of the contracting lattice. Contraction was calculated as percentage of the surface of the unreleased lattice. Data are shown as percentage of maximum contraction of vehicle control.

2.4. ECM production assay

Cells were seeded onto 96-well, optical, flat-bottom, black microplates (Nunc, Fisher Scientific) at 5×10^3 cells/well. After overnight attachment, they were stimulated with or without 10 ng/ml TGF-β1 and/or

compounds for 7 d. DRAQ5 in PBS (1:1000) was added, and cells were incubated for 5 min at 37 °C, 5% CO_2, before scanning the plate to obtain nuclear staining. Cells were then lysed using ammonium hydroxide as described previously [17], and ECM was fixed using a solution containing 50% methanol and 7.5% acetic acid for 1 h at–20 °C. Afterwards, ECM was stained with either Coomassie Blue (total ECM) overnight at 4 °C or primary antibodies (collagen I, Abcam, Cambridge, United Kingdom; collagen III, Millipore; collagen V, Abcam; fibronectin, Millipore, Burlington, Massachusetts, United States) at 1:1000 for 1 h on a shaker, followed by incubation with secondary antibody and scanning of the plate using an infrared imaging system (Odyssey CLx imager; LI-COR) at both 700 and 800 nm wavelengths. Results were normalised to the cell number before lysis.

2.5. Animal treatment

The animal model for PD was first described by El-Sakka et al. [18] and modified by Bivalacqua et al. [19]. Male Sprague-Dawley rats (10–12-wk old) were housed in a regulated environment with a 12-h light/dark cycle in a standard experimental laboratory. The animals had free access to food and water ad libitum. Fifty male Sprague-Dawley rats were divided into five groups: A: sham (injection of vehicle citrate buffer); B: TGF-β1 injection (1 μg in 100 μl citrate buffer [10 mM; Sigma-Aldrich]); C: TGF-β1 injection + tamoxifen (5 mg/kg/d; i.p.); D: TGF-β1 injection + vardenafil (1.5 mg/kg/d; drinking water); and E: TGF-β1 injection + tamoxifen + vardenafil. Treatment was initiated the next day after injury and continued for 5 wk followed by a 48 h washout period.

2.6. Assessment of erectile function

At the end of wash-off period, under ketamine (100 mg/kg) and xylazine (10 mg/kg) anaesthesia, the major pelvic ganglion (MPG) and cavernous nerve (CN) were exposed bilaterally via midline laparotomy. A 25 G butterfly needle, filled with 250 U/ml heparin solution, was inserted into the proximal left corpus cavernosum and connected to a pressure transducer for intracavernous pressure (ICP) measurement. The ICP was recorded at a rate of 25 samples per second. A bipolar stainless-steel hook electrode was used to stimulate the CN directly via a signal generator and a custom-built constant-current amplifier generating monophasic rectangular pulses with stimuli of 5, 7.5, 10, and 15 V. Depending on the anatomical positioning and accessibility of the nerve, stimulations were performed on either the left or the right MPG/CN. The maximal amplitude of ICP during nerve electrostimulation was calculated from baseline value and included for statistical analysis in each animal.

Systemic blood pressure was recorded by inserting PE-50 polyethylene tubing into the right common carotid artery. After functional testing, animals were euthanised by cervical dislocation. Following these measurements, the penis was harvested for histological, molecular, and transcriptional analysis.

2.7. Quantitative polymerase chain reaction

The High-Capacity cDNA Reverse Transcription Kit (Applied Biosystems, Foster City, California, United States) was used according to the manufacturer's instructions to transcribe RNA to cDNA. One microgram in 10 μl was added to 10 μl of the master mix for reverse transcription (RT) for a total reaction volume of 20 μl. After RT, cDNA was diluted 1:10 for quantitative polymerase chain reaction (qPCR). The Applied Biosystems TaqMan Fast Advanced Master Mix was used for qPCR. Gene-specific primer pairs for GAPDH, beta-actin, α-SMA, elastin, and collagens I, III, and V were purchased from Applied Biosystems. StepOnePlus Real-Time PCR System and software were used for the experiments and data analysis. Data were analysed using the $2^{-\Delta\Delta Ct}$ method for relative quantifications.

2.8. Western blot

Protein (20–30 μg) was mixed in a 1:1 ratio with 2× Laemmli buffer (Bio-Rad, Hercules, California, United States) under reducing or nonreducing conditions, and heat denatured at 95 °C for 4 min. Samples were loaded onto an Any kD Mini-PROTEAN TGX Precast Protein Gel (Bio-Rad) along with 5 μl of a protein ladder (Bio-Rad). After the gel electrophoresis, the transfer onto a methanol-activated PVDF membrane (Bio-Rad) was achieved by wet blotting for 1 h at 350 mA. Membranes were washed before blocking the unspecific binding with 10% (w/v) nonfat dried milk (NFDM; Marvel, Premier Foods, St. Albans, Hertfordshire, United Kingdom) in 0.1% Tris-buffered saline with Tween 20 (TBS-T) for 1 h. Primary antibodies were diluted in 5% NFDM in 0.1% TBS-T and incubated overnight at 4 °C on a shaker. Subsequently, membranes were washed 4× with 0.1% TBS-T and blocked again. After this, the secondary antibodies were added in a dilution of 1:3000 in 5% NFDM with 0.1% TBS-T and incubated for 1 h on a shaker in the dark. Four 5 minutes washes with 0.1% TBS-T were followed with 5-min incubation of an enhancer solution (SuperSignal West Dura; Thermo Fisher). Blots were visualised using a Syngene documentation system and Genesys software.

2.9. Statistical analysis

Data analysis was performed using Microsoft Excel 2013 or GraphPad Prism 7 software. The differences between multiple groups in in vivo RT-qPCR and Western blot quantification experiments were compared using one-way analysis of variance (ANOVA). The differences between multiple groups in ICP/MAP and the in vitro in-cell enzyme-linked immunosorbent assay (ICE) synergy experiments were compared using two-way ANOVA. Student t test for unpaired means (two sided) was used to compare the difference between two groups in in vitro ICC and RT-qPCR experiments. Prior to performing this calculation, F test of equality of variances was performed, to ensure that equal variance could be assumed when performing Student t test. A p value of <0.05 was considered statistically significant. All in vitro experiments were performed at least in triplicate ($n = 9$) using samples from three patients ($N = 3$). Results from the nine experiments were pooled, and the mean values and standard errors of mean were used for statistical analysis. Eight rats were used in each group in in vivo experiments. Results from the rats in each group were pooled, and the mean values and standard errors of mean were used for statistical analysis.

Z factor (Z') was used to measure the statistical effect size of TGF-β1–induced myofibroblast transformation, to evaluate its reproducibility, variability, and potential use as a high-throughput screening assay. The formula for Z' factor is given in the Supplementary material.

3. Results

3.1. Development and validation of the phenotypic assay

We have isolated primary fibroblasts from the plaque and nonplaque TA of patients with PD. We also isolated primary fibroblasts from TA of patients with penile cancer as nonfibrotic controls (Supplementary Fig. 1). The primary fibroblasts were similar in morphology and function (as shown by their response to TGF-β1) in all three groups: fibroblasts derived from the plaque of PD patients, fibroblasts derived from the nonplaque TA of PD patients, and fibroblasts derived from the TA of patients with penile cancer. Based on this similarity, we have utilised fibroblasts derived from the nonplaque TA of PD patients throughout this work since they would be more representative of

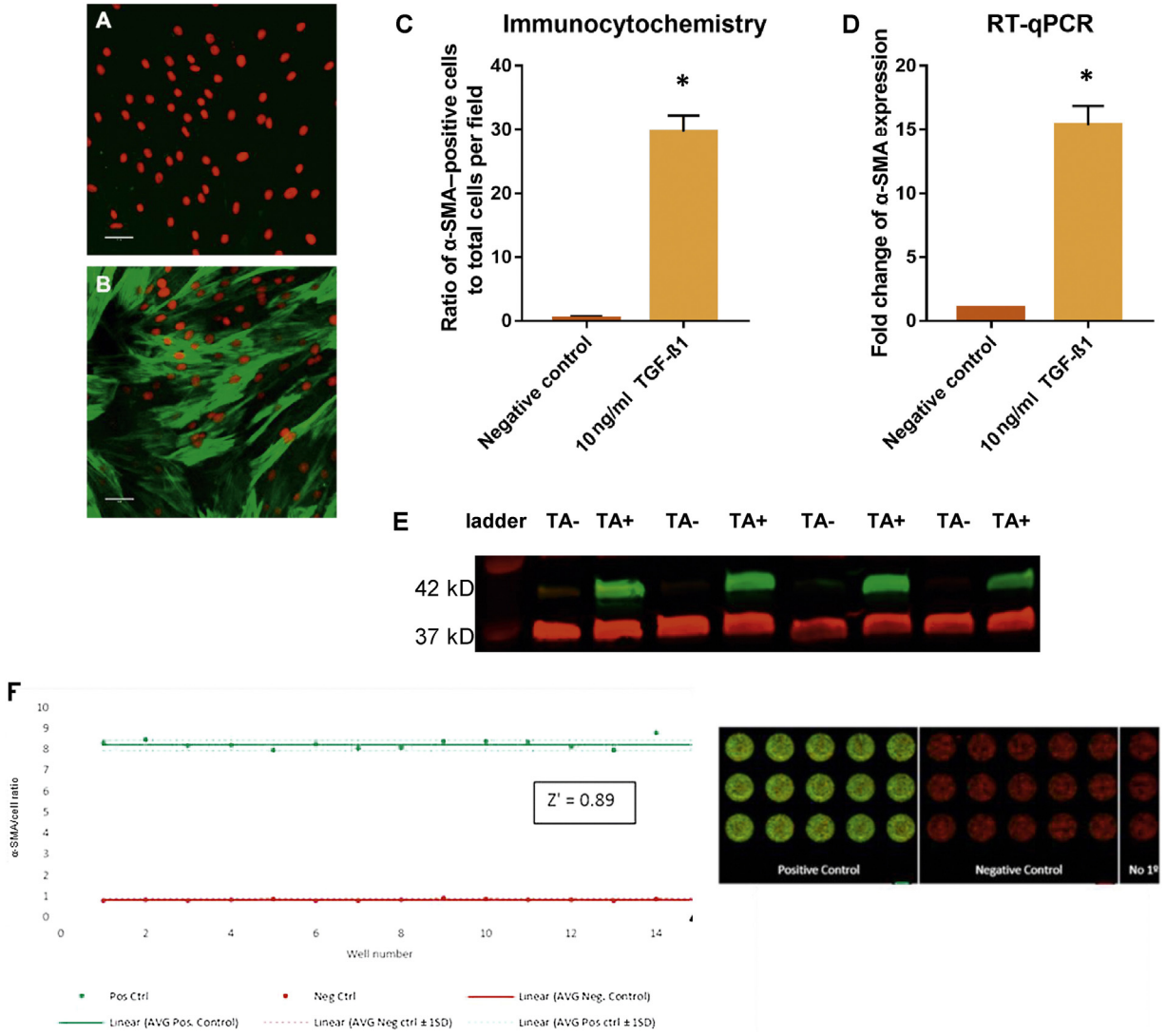

Fig. 1 – TGF-β1 induces myofibroblast transformation that can be measured by a high-throughput screening assay. Fibroblasts were exposed to TGF-β1 (10 ng/ml) for 72 h. Representative images of α-SMA staining in (A) untreated TA-derived cells and (B) TA-derived cells exposed to TGF-β1. Images were captured at 200× magnification. Scale bars: 50 μm. (C) Quantification of α-SMA–positive cells. (D) The mRNA levels of α-SMA were determined using the $2^{-\Delta\Delta Ct}$ method. Data points were plotted as mean ± SEM ($N = 3$ patients for each group; $n = 9$). (E) Representative Western blot for α-SMA content in protein lysates from untreated cells and cells exposed to 10 ng/ml TGF-β1 for 72 h: 20 μg of protein was loaded under reducing conditions. Lower bands (35 kD) represent GAPDH loading control, higher bands (42 kD) represent α-SMA. Lane 1: protein ladder; lanes 2, 4, 6, 8: untreated TA-derived cells; lanes 3, 5, 7, 9: cells exposed to 10 ng/ml TGF-β1. (F) Statistical validation of the ICE method. Positive controls correspond to wells exposed to TGF-β1; negative controls correspond to wells exposed to media only. Data were normalised to nuclear dye intensity. Validation for high-throughput screening by calculation of Z' comparing negative with positive control wells, yielding a Z' value of 0.89. α-SMA = alpha-smooth muscle actin; AVG = average; Ctrl = control; ICE = in-cell enzyme-linked immunosorbent assay; Neg = negative; Pos = positive; RT-qPCR = reverse transcription quantitative polymerase chain reaction; SEM = standard error of the mean; TA = tunica albuginea; TGF-β1 = transforming growth factor-β1.* $p < 0.05$ versus negative control.

fibroblasts that have not been exposed to a profibrotic environment. The fibroblast identity of the TA-derived cells was validated (Supplementary Fig. 2).

Upon exposure toTGF-β1 (10 ng/ml for 72 h), we observed a significant eight-fold increase in α-SMA expression in both mRNA and protein levels in TA-derived fibroblasts (Fig. 1). We then developed a phenotypic screening assay in a 96-well plate format using ICE where the cell viability and α-SMA protein expression can be measured simultaneously in a reproducible manner (-Z' = 0.89; Fig. 1). The assay was further validated using vehicle control and a TGF-β1 receptor antagonist (SB505124) where the cells remained viable in up to 1% dimethyl sulphoxide and SB505124 inhibited TGF-β1–induced myofibroblast transformation in a concentration-dependent manner (IC50 = 0.6 μM; Supplementary Fig. 3).

3.2. *Hit identification*

We then tested 21 compounds/drugs (Supplementary Table 1), which have been suggested to be efficacious in PD based on in vitro and in vivo studies and/or early-phase clinical studies. Out of these 21 drugs, only two classes, SERMs and PDE5i, showed significant inhibition of myofi-

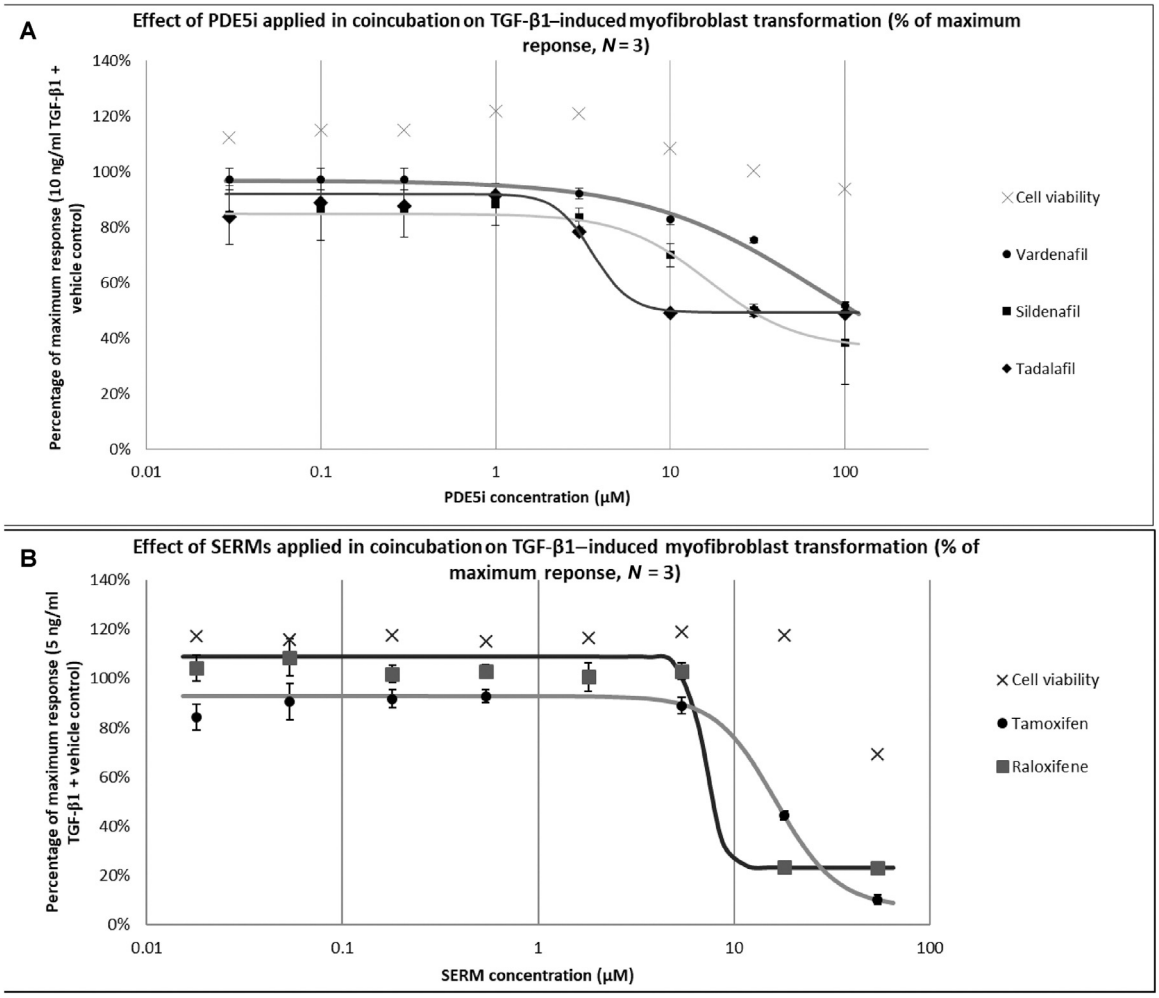

Fig. 2 – Concentration response curves for hits acquired from screening campaign. Effect of the (A) PDE5i vardenafil, sildenafil, and tadalafil and (B) SERMs tamoxifen and raloxifen on TGF-β1–induced myofibroblast transformation. Cells derived from TA tissue were exposed to a range of concentrations of PDE5i between 0.03 and 100 μM in coincubation with 10 ng/ml TGF-β1 for 72 h. Data points were plotted as average ± SEM of the percentage of maximum response of the α-SMA/DNA staining ratio (*N* = 3; *n* = 9). PDE5i = phosphodiesterase type 5 inhibitors; SEM = standard error of the mean; SERM = selective oestrogen receptor modulator; TGF-β1 = transforming growth factor-β1.

broblast transformation. Full concentration response curves were constructed for these hits, which yielded inverse sigmoid curves with an upper and a lower plateau without affecting the cell viability (Fig. 2). The following molecules were used to investigate the two classes of drugs: vardenafil, sildenafil, and tadalafil as PDE5i (IC_{50} = 30, 15, and 3.5 μM, respectively), and tamoxifen and raloxifene as SERMs (IC_{50} = 11.9 and 7 μM, respectively). When a PDE5i (vardenafil) and a SERM (tamoxifen) were tested in combination, a synergy between the two drugs became apparent (the observed inhibition was greater than the arithmetic sum of each; Fig. 2 and Supplementary Table 2).

3.3. *Functional assays*

The two classes of drugs were then tested in functional assays. Firstly, we tested their efficacy in inhibiting collagen gel contraction as a measure of myofibroblast contractility—a characteristic function of myofibroblasts, which separates them from fibroblasts. Collagen gels were loaded with fibroblasts, and contraction was measured after stimulation with TGF-β1 as described before [20,21]. Both vardenafil and tamoxifen inhibited TGF-β1–induced contraction of collagen at concentrations of 10 and 1 μM, respectively (Fig. 3). Secondly, we tested the drugs' efficacy in inhibiting ECM protein production, which is again one of the critical characteristic functions of myofibroblasts. Again, both vardenafil and tamoxifen inhibited TGF-β1–induced ECM protein production (collagens I, III, and V and fibronectin; IC_{50} = 23, 17, 23, and 44 μM for vardenafil, and 7, 5.3, 6.7, and 1.6 μM for tamoxifen, respectively; Fig. 4).

3.4. *In vivo testing of the two hits*

To elucidate whether the drugs could also prevent fibrosis in vivo, they were taken further to be tested in an animal model for PD. Five weeks after TGF-β1 injection into the rat TA, with or without treatment with vardenafil, tamoxifen, or their combination, the rats were subjected to erectile function measurement (ICP measurement) before harvest-

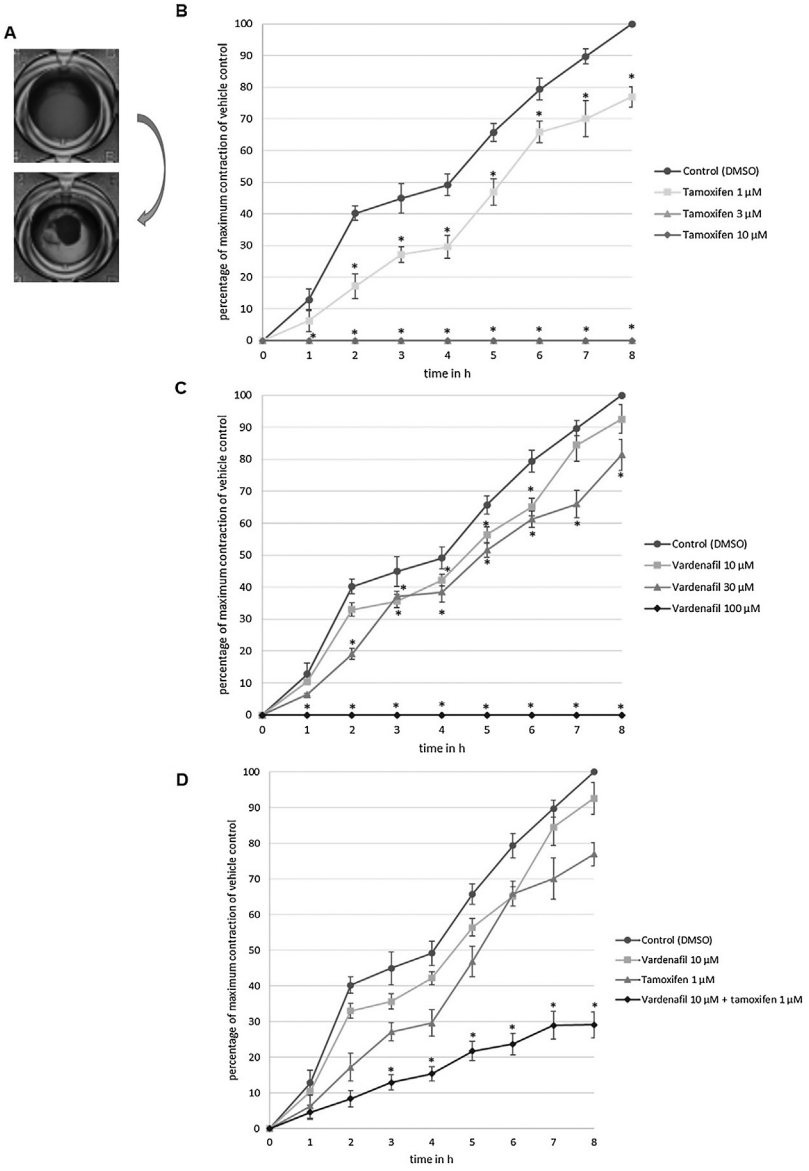

Fig. 3 – Effect of compounds on TGF-β1–induced myofibroblast collagen contraction in fibroblast-populated collagen lattices (FPCLs). (A) Representation of the contraction of the fibroblast-populated collagen lattices. Top row: example for no contraction after release. Bottom row: example for uniform contraction after release from the wall of the well. FPCLs were exposed to (B) 10 ng/ml TGF-β1 and various concentrations of tamoxifen or (C) vardenafil. FPCLs were released after 72 h and contraction was observed for 8 h. Data were presented as percentage of maximum collagen contraction compared with vehicle control (DMSO) in cells exposed to tamoxifen/vardenafil. Data points were plotted as mean ± SEM (*N* = 3; *n* = 9). DMSO = dimethyl sulphoxide; SEM = standard error of the mean; TGF-β1 = transforming growth factor-β1.* $p < 0.05$ versus vehicle control at the same time point.

ing the penis for molecular analysis. The ICP measurement revealed that TGF-β1 injection led to a decrease in erectile function by 55%, which was prevented in all treatment groups. Treatment groups showed no significant differences in ICP compared with the vehicle-injected group (Fig. 5). Subsequent mRNA expression analysis of the penile tissue harvested from the rats showed that expression of collagens I, III, and V were significantly upregulated in the TGF-β1 injection group, but not in the vehicle or treated groups. Treatment with vardenafil or tamoxifen therefore prevented upregulation of TGF-β1–induced increase in collagen expression. Interestingly, the combination of vardenafil and tamoxifen acted synergistically on the downregulation of elastin (Fig. 5). The formation of fibrosis in response to TGF-β1 injection into the penis was further confirmed by measuring α-SMA in the corpus cavernosum (as a measure of loss of smooth muscle mass due to fibrotic tissue) using Western blot and immunohistochemistry. The results showed a significant loss of smooth muscle, which was prevented in the treatment groups (Fig. 5). Furthermore, immunohistochemistry using haematoxylin and eosin and Masson's Trichrome staining showed increased infiltration of inflammatory cells, formation of fibrosis, and loss of smooth muscle in the TGF-β1–injected group, effects that were prevented in the treatment groups (Fig. 6).

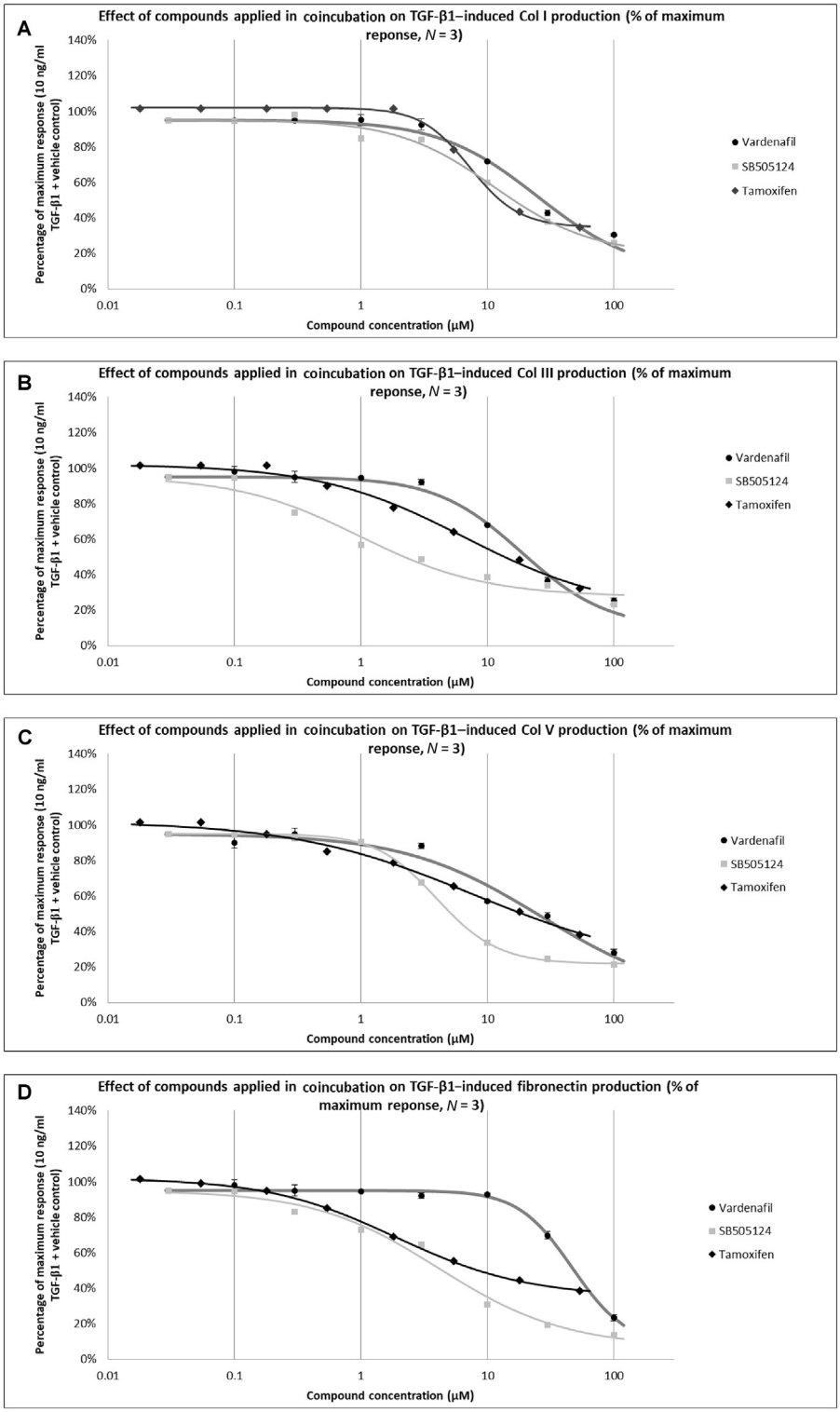

Fig. 4 – Effect of compounds on TGF-β1–induced myofibroblast ECM production. Cells derived from TA tissue were exposed to a range of concentrations of vardenafil, tamoxifen, or SB505124 in coincubation with 10 ng/ml TGF-β1 for 7 d. ECM was stained for (A) collagen I (Col I), (B) collagen III (Col III), (C) collagen V (Col V), and (D) fibronectin after cell lysis. Data points were plotted as average ± SEM of the percentage of maximum response of protein/prelysis DNA staining ratio (*N* = 3; *n* = 9). ECM = extracellular matrix; SEM = standard error of the mean; TA = tunica albuginea; TGF-β1 = transforming growth factor-β1.

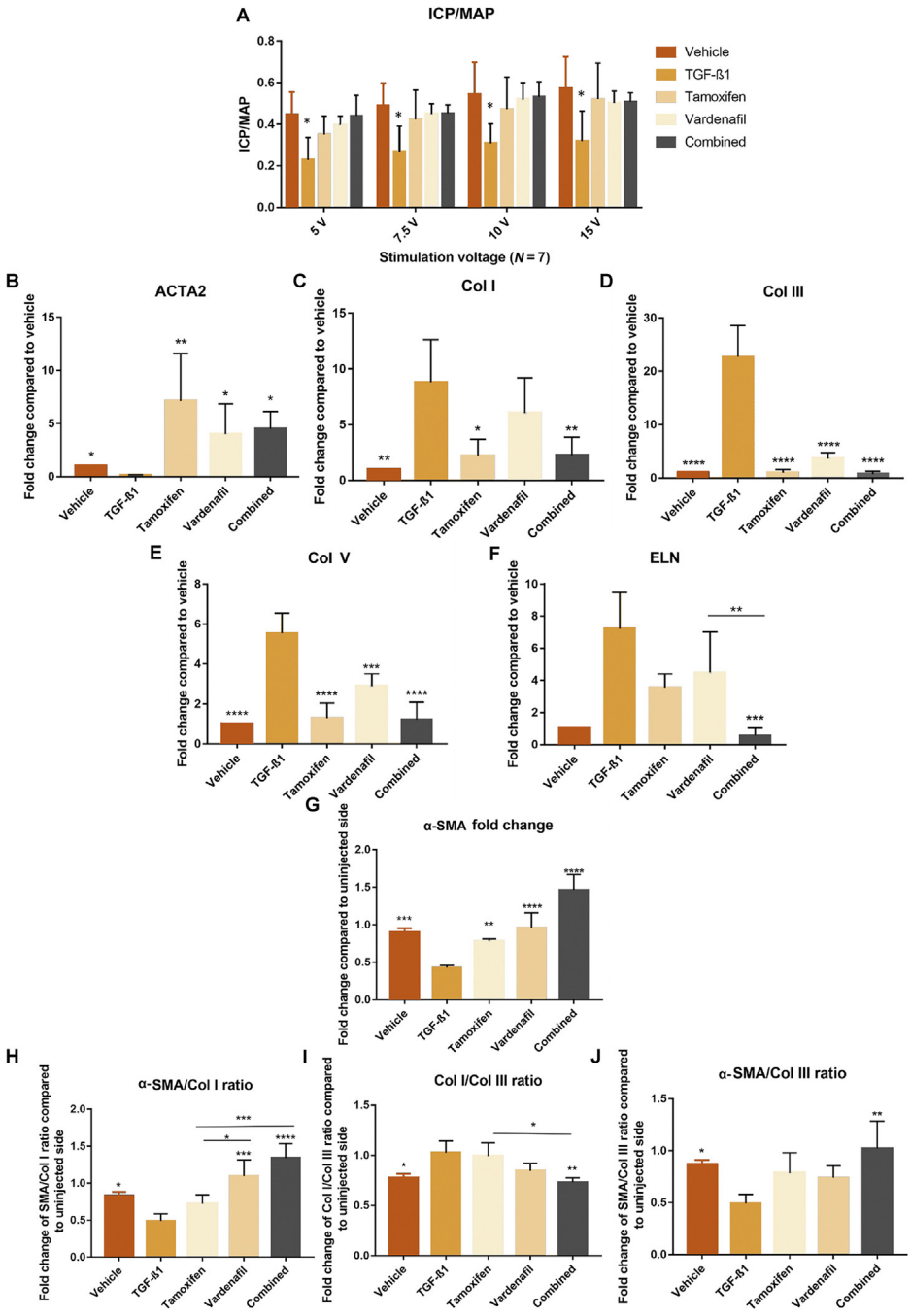

Fig. 5 – Vardenafil, tamoxifen, and their combination ameliorate penile fibrosis in an animal model for PD. (A) ΔICP measurement for different stimulation voltages in all the treatment groups. Intracavernous pressure (ICP) change from baseline to peak ICP (ΔICP). Data were plotted as mean ± SEM ($N = 7$). * $p < 0.05$ versus vehicle-injected group. (B) mRNA levels of α-SMA (ACTA2) were determined using the $2^{-\Delta\Delta Ct}$ method. Data points were plotted as mean ± SEM ($N = 4$). * $p < 0.05$, ** $p < 0.01$ versus TGF-β1–injected group. (C) mRNA levels of Col I were determined using the $2^{-\Delta\Delta Ct}$ method. Data points were plotted as mean ± SEM ($N = 4$). * $p < 0.05$, ** $p < 0.01$ versus TGF-β1–injected group. (D) mRNA levels of Col III were determined using the $2^{-\Delta\Delta Ct}$ method. Data points were plotted as mean ± SEM ($N = 4$). **** $p < 0.0001$ versus TGF-β1-injected group. (E) mRNA levels of Col V were determined using the $2^{-\Delta\Delta Ct}$ method. Data points were plotted as mean ± SEM ($N = 4$). *** $p = 0.0001$, **** $p < 0.0001$ versus TGF-β1-injected group. (F) mRNA levels of elastin (ELN) were determined using the $2^{-\Delta\Delta Ct}$ method. Data points were plotted as mean ± SEM ($N = 4$). ** $p < 0.001$ vardenafil versus combination. *** $p = 0.0001$ versus TGF-β1-injected group. (G) Western blot quantification of α-SMA. Data were shown as fold change between injected and uninjected sides of the penis. Data points were plotted as mean ± SEM ($N = 3$). ** $p < 0.001$, ** $p < 0.001$, *** $p = 0.0001$ versus TGF-β1-injected group. (H) Western blot quantification of α-SMA/Col I ratio. Data were shown as a ratio of fold change between injected and uninjected sides of the penis for α-SMA and Col I. Data points were plotted as mean ± SEM ($N = 3$). * $p < 0.05$, *** $p = 0.0001$, **** $p < 0.0001$ versus TGF-β1–injected group or in between groups. (I) Western blot quantification of Col I/Col III ratio. Data were shown as a ratio of fold change between injected and uninjected sides of the penis for Col I and Col III. Data points were plotted as mean ± SEM ($N = 3$). * $p < 0.05$, ** $p < 0.001$ versus TGF-β1–injected group or in between groups. (J) Western blot quantification of α-SMA/Col III ratio. Data were shown as a ratio of fold change between injected and uninjected sides of the penis for α-SMA and Col III. Data points were plotted as mean ± SEM ($N = 3$). * $p < 0.05$, ** $p < 0.001$ versus TGF-β1–injected group or in between groups. α-SMA = alpha-smooth muscle actin; Col = collagen; combined = TGF-β1 injected plus combined treatment group; MAP = mean arterial pressure; PD = Peyronie's disease; SEM = standard error of the mean; tamoxifen = TGF-β1 injected + tamoxifen treatment group; TGF-β1 = transforming growth factor-β1; TGF-β1 = TGF-β1–injected group; vardenafil = TGF-β1 injected + vardenafil treatment group; vehicle = vehicle–injected group.

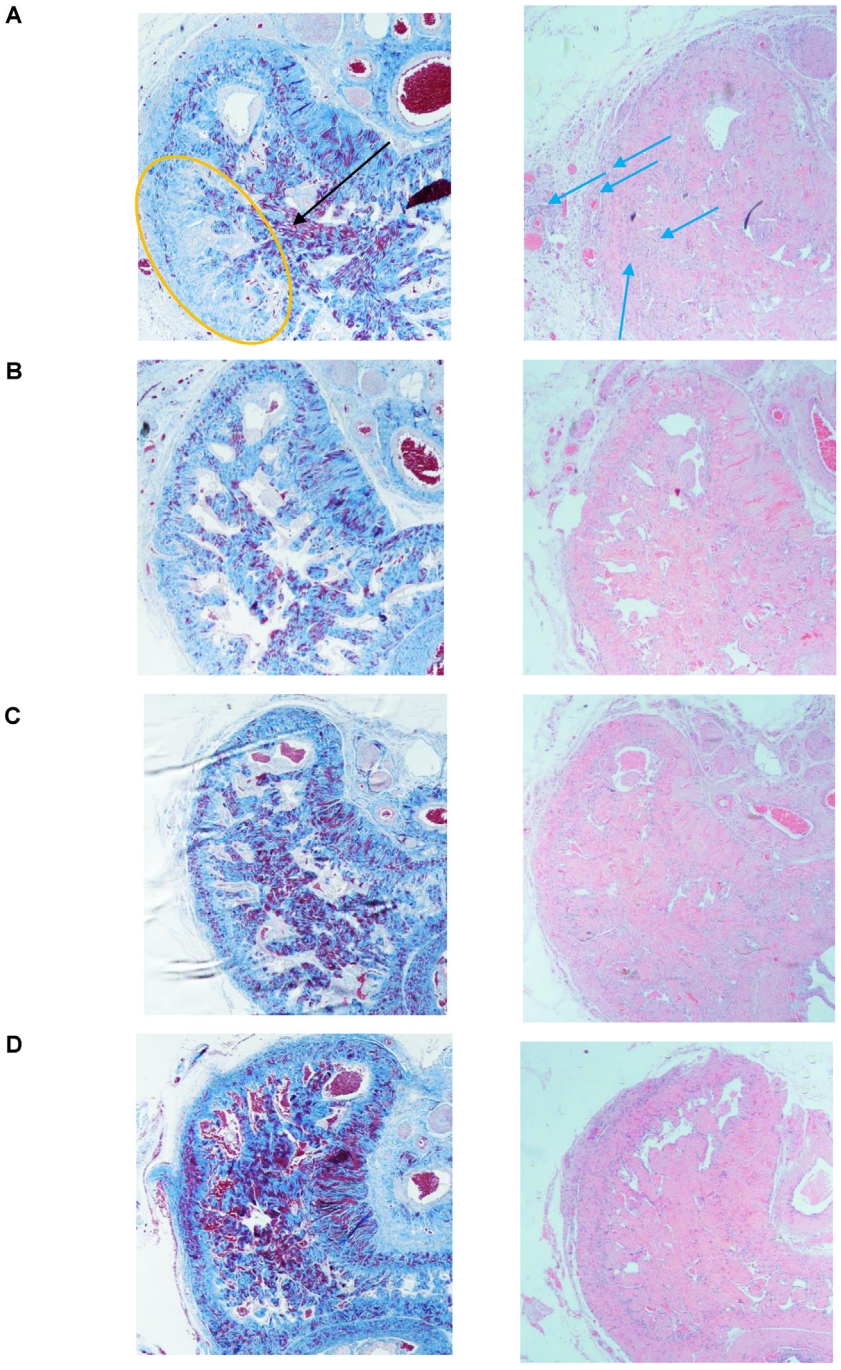

Fig. 6 – Immunohistochemical staining for different treatment groups. Representative images of Masson's Trichrome staining and H&E staining in whole sections of rat penis for (A) TGF-β1–injected group (left: Masson's Trichrome staining for injected side [4× magnification], right: H&E staining for injected side (4× magnification)], (B) TGF-β1–injected group treated with vardenafil (left: Masson's Trichrome staining for injected side [4× magnification], right: H&E staining for injected side [4× magnification]), (C) TGF-β1–injected group treated with tamoxifen (left: Masson's Trichrome staining for injected side [4× magnification], right: H&E staining for injected side [4× magnification]), and (D) TGF-β1–injected group treated with the combination of vardenafil and tamoxifen (left: Masson's Trichrome staining for injected side [4× magnification], right: H&E staining for injected side [4× magnification]). The black arrow indicates smooth muscle, the orange circle indicates collagenous fibrotic plaque, and blue arrows indicate nuclei (cellular infiltration due to inflammation). H&E = haematoxylin and eosin; TGF-β1 = transforming growth factor-β1.

4. Discussion

In contrast to the single-target approach, phenotypic screening seeks to find compounds that target a phenotype rather than a single molecular target. In this case, we have chosen transformation of fibroblasts to myofibroblasts as the target phenotype and developed an assay that can quantify inhibition of myofibroblast transformation in a reproducible manner. Using this assay, we then tested 21 compounds/drugs that have been suggested as potentially antifibrotic agents. Among this cohort, only two groups were able to inhibit myofibroblast transfor-

mation: PDE5i and SERMs. When applied together, these two classes showed synergistic activity both in vitro and in vivo.

To our knowledge, this is the first study to show a synergy between PDE5i and SERMs. PDE5i have previously been suggested to be effective antifibrotic agents in vitro using TA-derived fibroblasts [22]. This was further confirmed in an animal model for PD with long-term vardenafil treatment [23,24]. Furthermore, in vivo studies led to PDE5i being proposed as a potential treatment for other fibrotic disorders such as muscle fibrosis in a Duchenne muscular dystrophy mouse model [25], and for the prevention of cardiac fibrosis and its underlying cardiac fibroblast activation [26]. Tamoxifen has been shown to be effective in animal models for renal tubulointerstitial fibrosis and periportal hepatic fibrosis [27,28]. The antimyofibroblast effect has also been reported in models utilising TGF-β1–mediated activation of primary human dermal and breast fibroblasts [29]. Previous research suggested that the effect of tamoxifen on fibroblast-mediated collagen contraction is due either to downregulation of TGF-β2 [30] or a change in the morphology of fibroblasts [31]. Oestradiol has been shown to inhibit transformation of TA-derived fibroblast to myofibroblasts [32]. However, no previous study has investigated the effect of tamoxifen in an animal model of PD.

Previous clinical studies have shown mixed results using PDE5i and SERMs [33–37]. An open-label single-arm study with tamoxifen showed a positive effect [33], while a later placebo-controlled study showed no effect with tamoxifen [34]. However, the open-label study noted that tamoxifen showed some improvement in patients with early PD [33], while all the patients in the latter study were in the late phase of the disease [34]. Similarly, in studies with PDE5i, the results have been mixed [35–37]. This is not surprising since the drugs were tested on patients with established plaque-fibrotic tissue. Our results suggest that PDE5i or SERMs inhibit myofibroblast transformation and ECM production; they would not be able to reverse the established/preformed fibrosis. We are therefore proposing that the combination of PDE5i and SERMs will inhibit myofibroblast transformation, thereby leading to new fibrosis formation, and prevent new plaque formation.

We believe that more and more men are presenting at early stages of the disease, as there are now better information resources and access to healthcare to have symptoms investigated. Indeed, others have reported that 30–40% of patients present with progressing deformity [38–40]. This drug combination may be more effective in patients in the acute phase where penile pain or the onset of a nodule would be an indication for referral. This will be an area for patient and primary care education.

The doses of vardenafil and tamoxifen used in our animal model are representative of their clinical doses: tamoxifen 20 mg twice daily and vardenafil 20 mg daily (please see the Supplementary material that explains the rationale behind the dose selection).

This study is limited by not providing a mechanism of action for the proposed synergistic effect of the drugs, something that is currently being investigated. The number of compounds/drugs that have been screened also limits the study; other SERMs that are used in treatment of male fertility would be very interesting to test. A larger phenotypic screening campaign is planned, hopefully providing us with more hits that might reveal new treatment strategies not only for PD but also for fibrosis in general.

Another limitation to the study is that the drugs were tested in only one of the several animal PD models [41]. Although TGF-β1 injection model is most widely used, it may not necessarily be the most clinically relevant animal model; for example, it does not develop curvature of the penis. Further studies are required to test this combination in other animal models of PD.

5. Conclusions

In summary, this is the first study to demonstrate a synergistic antifibrotic effect of a combination of PDE5i and SERMs in in vitro and in vivo disease models. Future prospective clinical trials using a combination of these drugs should be considered during the active phase of PD, given the early evidence of benefit in both in vitro and in vivo models. We also envisage that the combination will be more efficacious than using either of the drugs as a monotherapy. We will be investigating such a combination in men with early PD in the near future. These results are likely to lead to further research into the interaction between the two pathways and development of novel therapeutic approaches for the prevention and/or treatment of other fibrotic diseases.

Author contributions: Selim Cellek had full access to all the data in the study and takes responsibility for the integrity of the data and the accuracy of the data analysis.

Study concept and design: Cellek, Mateus, Stebbeds, Ilg.
Acquisition of data: Ilg, Mateus, Stebbeds, Milenkovic.
Analysis and interpretation of data: Cellek, Ilg, Mateus, Stebbeds, Albersen.
Drafting of the manuscript: Ilg, Mateus, Stebbeds, Christopher, Milenkovic, Albersen, Muneer, Ralph, Cellek.
Critical revision of the manuscript for important intellectual content: Ilg, Mateus, Stebbeds, Christopher, Milenkovic, Albersen, Muneer, Ralph, Cellek.
Statistical analysis: Cellek, Mateus, Stebbeds, Ilg.
Obtaining funding: Cellek, Ralph, Albersen.
Administrative, technical, or material support: Cellek, Mateus, Stebbeds, Ilg.
Supervision: Cellek, Albersen.
Other: None.

Financial disclosures: Selim Cellek certifies that all conflicts of interest, including specific financial interests and relationships and affiliations relevant to the subject matter or materials discussed in the manuscript (eg, employment/affiliation, grants or funding, consultancies, honoraria, stock ownership or options, expert testimony, royalties, or patents filed, received, or pending), are the following: None.

***Funding/Support and role of the sponsor*:** This study was partly funded by the European Society for Sexual Medicine. Asif Muneer is supported by the NIHR Biomedical Research Centre, University College London Hospital.

Appendix A. Supplementary data

Supplementary data associated with this article can be found, in the online version, at https://doi.org/10.1016/j.eururo.2018.10.014.

References

[1] Schwarzer U, Sommer F, Klotz T, Braun M, Reifenrath B, Engelmann U. The prevalence of Peyronie's disease: results of a large survey. BJU Int 2001;88:727–30.
[2] Hellstrom WJG. History, epidemiology, and clinical presentation of Peyronie's disease. Int J Impot Res 2003;15:S91–2.
[3] Nelson CJ, Diblasio C, Kendirci M, Hellstrom W, Guhring P, Mulhall JP. The chronology of depression and distress in men with Peyronie's disease. J Sex Med 2008;5:1985–90.
[4] Egui Rojo MA, Moncada Iribarren I, Carballido Rodriguez J, Martinez-Salamanca JI. Experience in the use of collagenase *Clostridium histolyticum* in the management of Peyronie's disease: current data and future prospects. Ther Adv Urol 2014;6:192–7.
[5] Andrews HO, Al-Akraa M, Pryor JP, Ralph DJ. The Nesbit operation for Peyronie's disease: an analysis of the failures. BJU Int 2002;87:658–60.
[6] McAnulty RJ. Fibroblasts and myofibroblasts: their source, function and role in disease. Int J Biochem Cell Biol 2007;39:666–71.
[7] Hinz B, Phan SH, Thannickal VJ, Galli A, Bochaton-Piallat M-L, Gabbiani G. The myofibroblast: one function, multiple origins. Am J Pathol 2007;170:1807–16.
[8] Borthwick LA, Wynn TA, Fisher AJ. Cytokine mediated tissue fibrosis. Biochim Biophys Acta 2013;1832:1049–60.
[9] McAnulty RJ, Campa JS, Cambrey AD, Laurent GJ. The effect of transforming growth factor β on rates of procollagen synthesis and degradation in vitro. Biochim Biophys Acta 1991;1091:231–5.
[10] Guyot C, Lepreux S, Combe C, et al. Hepatic fibrosis and cirrhosis: the (myo)fibroblastic cell subpopulations involved. Int J Biochem Cell Biol 2006;38:135–51.
[11] Ask K, Martin GEM, Kolb M, Gauldie J. Targeting genes for treatment in idiopathic pulmonary fibrosis. Challenges and opportunities, promises and pitfalls. Proc Am Thorac Soc 2006;3:389–93.
[12] Nandhini T. Molecular mechanism in renal fibrosis—a review. J Pharm Sci Res 2014;6:334–7.
[13] Jalkut M, Gonzalez-Cadavid N, Rajfer J. New discoveries in the basic science understanding of Peyronie's disease. Curr Urol Rep 2004;5:478–84.
[14] Gelfand RA, Vernet D, Kovanecz I, Rajfer J, Gonzalez-Cadavid NF. The transcriptional signatures of cells from the human Peyronie's disease plaque and the ability of these cells to generate a plaque in a rat model suggest potential therapeutic targets. J Sex Med 2015;12:313–27.
[15] Bollong MJ, Yang B, Vergani N, et al. Small molecule-mediated inhibition of myofibroblast transdifferentiation for the treatment of fibrosis. Proc Natl Acad Sci U S A 2017;114:4679–84.
[16] Mateus M, Ilg MM, Stebbeds WJ, et al. Understanding the role of adenosine receptors in the myofibroblast transformation in Peyronie's disease. J Sex Med 2018;15:947–57.
[17] Fisher M, Jones RA, Huang L, et al. Modulation of tissue transglutaminase in tubular epithelial cells alters extracellular matrix levels: a potential mechanism of tissue scarring. Matrix Biol 2009;28:20–31.
[18] El-Sakka AI, Hassoba HM, Chui RM, Bhatnagar RS, Dahiya R, Lue TF. An animal model of Peyronie's-like condition associated with an increase of transforming growth factor beta mRNA and protein expression. J Urol 1997;158:2284–90.
[19] Bivalacqua TJ, Diner EK, Novak TE, et al. A rat model of Peyronie's disease associated with a decrease in erectile activity and an increase in inducible nitric oxide synthase protein expression. J Urol 2000;163:1992–8.
[20] Bell E, Ivarsson B, Merrill C. Production of a tissue-like structure by contraction of collagen lattices by human fibroblasts of different proliferative potential in vitro. Proc Natl Acad Sci 1979;76:1274–8.
[21] Dallon JC, Ehrlich HP. A review of fibroblast-populated collagen lattices. Wound Repair Regen 2008;16:472–9.
[22] Valente EGA, Vernet D, Ferrini MG, Qian A, Rajfer J, Gonzalez-Cadavid NF. L-arginine and phosphodiesterase (PDE) inhibitors counteract fibrosis in the Peyronie's fibrotic plaque and related fibroblast cultures. Nitric Oxide 2003;9:229–44.
[23] Ferrini MG, Kovanecz I, Nolazco G, Rajfer J, Gonzalez-Cadavid NF. Effects of long-term vardenafil treatment on the development of fibrotic plaques in a rat model of Peyronie's disease. BJU Int 2006;97:625–33.
[24] Gonzalez-Cadavid NF, Rajfer J. Treatment of Peyronie's disease with PDE5 inhibitors: an antifibrotic strategy. Nat Rev Urol 2010;7:215–21.
[25] Nio Y, Tanaka M, Hirozane Y, et al. Phosphodiesterase 4 inhibitor and phosphodiesterase 5 inhibitor combination therapy has antifibrotic and anti-inflammatory effects in MDX mice with Duchenne muscular dystrophy. FASEB J 2017;31:5307–20.
[26] Gong W, Yan M, Chen J, Chaugai S, Chen C, Wang D. Chronic inhibition of cyclic guanosine monophosphate-specific phosphodiesterase 5 prevented cardiac fibrosis through inhibition of transforming growth factor β-induced Smad signaling. Front Med 2014;8:445–55.
[27] Kim D, Lee AS, Jung YJ, et al. Tamoxifen ameliorates renal tubulointerstitial fibrosis by modulation of estrogen receptor α-mediated transforming growth factor-β1/Smad signaling pathway. Nephrol Dial Transplant 2014;29:2043–53.
[28] Ryu SH, Chung YH, Lee JK, et al. Antifibrogenic effects of tamoxifen in a rat model of periportal hepatic fibrosis. Liver Int 2009;29:308–14.
[29] Carthy JM, Sundqvist A, Heldin A, et al. Tamoxifen inhibits TGF-β-mediated activation of myofibroblasts by blocking non-Smad signaling through ERK1/2. J Cell Physiol 2015;230:3084–92.
[30] Kuhn MA, Wang X, Payne WG, Ko F, Robson MC. Tamoxifen decreases fibroblast function and downregulates TGFβ2 in Dupuytren's affected palmar fascia. J Surg Res 2002;103:146–52.
[31] Hu D, Hughes MA, Cherry GW. Topical tamoxifen—a potential therapeutic regime in treating excessive dermal scarring? Br J Plast Surg 1998;51:462–9.
[32] Jiang HS, Zhu LL, Zhang Z, Chen H, Chen Y, Dai YT. Estradiol attenuates the TGF-β1-induced conversion of primary TAFs into myofibroblasts and inhibits collagen production and myofibroblast contraction by modulating the Smad and Rho/ROCK signaling pathways. Int J Mol Med 2015;36:801–7.
[33] Ralph DJ, Brooks MD, Bottazoo GF, Pryor JP. The treatment of Peyronie's disease with tamoxifen. Br J Urol 1992;70:648–51.
[34] Teloken C, Rhoden EL, Grazziotin TM, Teodósio Da Ros C, Sogari PR, Souto CAV. Tamoxifen versus placebo in the treatment of Peyronie's disease. J Urol 1999;162:2003–5.
[35] Dell'Atti L. Tadalafil once daily and intralesional verapamil injection: a new therapeutic direction in Peyronie's disease. Urol Ann 2015;7:345–9.

[36] Ozturk U, Yesil S, Goktug HNG, et al. Effects of sildenafil treatment on patients with Peyronie's disease and erectile dysfunction. Irish J Med Sci 2014;183:449–53.
[37] Park TY, Jeong HG, Park JJ, et al. The efficacy of medical treatment of Peyronie's disease: potassium para-aminobenzoate monotherapy vs. combination therapy with tamoxifen, L-carnitine, and phosphodiesterase type 5 inhibitor. World J Mens Health 2016;34:40–6.
[38] Kadioglu A, Tefekli A, Erol B, Oktar T, Tunc M, Tellaloglu S. A retrospective review of 307 men with Peyronie's disease. J Urol 2002;168:1075–9.
[39] Mulhall JP, Schiff J, Guhring P. An analysis of the natural history of Peyronie's disease. J Urol 2006;175:2115–8.
[40] Berookhim BM, Choi J, Alex B, Mulhall JP. Deformity stabilization and improvement in men with untreated Peyronie's disease. BJU Int 2014;113:133–6.
[41] Stebbeds W, Cellek S, Ralph D. Solving a bottleneck in animal models of Peyronie's disease. Asian J Androl 2014;16:639.